

# Pristimerin improve renal fibrosis by regulating miRNA-145-5p *in vitro* and *in vivo* study

Chen XIAO-MEI<sup>1</sup>, Zhang JIN-YU<sup>1</sup>, Yang YAN-LANG, Wang YU-WEI<sup>1</sup>, Yu YUAN-YUAN<sup>1</sup>, Xu HAI-HONG<sup>1\*</sup> 

## Abstract

Pristimerin (Pri) was a kind of extraction from natural plant, and it has anti-inflammation effects in previous studies, however, it has been unclear that Pri's effect in renal fibrosis treatment. The purpose of this research was to evaluate pristimerin (Pri) treatment effects in renal fibrosis and relative mechanisms *in vivo* study. Using UUO and TGF- $\beta$ 1 to make renal fibrosis rats and HK-2 cell fibrosis model. Evaluating renal tissues pathological and fibrosis by HE and Masson staining; measuring Scr and BUN concentrations of serum, IL-1 $\beta$ , TNF- $\alpha$ , SOD and MDA concentrations by ELISA assay in serum and supernatant. Relative gene expressions were measured by RT-qPCR assay in renal tissues and cells and relative proteins expression by WB assay. Using Double luciferase assay to analysis correlation between miRNA-145-5p and TLR4. NF- $\kappa$ B(p65) nuclear volume were evaluated by cellular immunofluorescence. Scr, BUN, IL-1 $\beta$ , TNF- $\alpha$  and MDA concentrations were significantly increased and SOD concentration was significantly down-regulation ( $P < 0.001$ ) in Model rats group; miRNA-145-5p gene expression was significantly depressed, TLR4, MyD88 and NF- $\kappa$ B(p65) gene expressions were significantly increased ( $P < 0.001$ , respectively); with Pri supplement, the renal pathological, masson region, Scr, BUN, IL-1 $\beta$ , TNF- $\alpha$ , SOD and MDA were significantly improved. In cell experiment, miRNA-145-5p play important role in Pri treatment of renal fibrosis by targeting TLR4. Pri could improve renal fibrosis by via regulation miRNA-145-5p to target TLR4.

**Keywords:** pristimerin; renal fibrosis; miRNA-145-5p; TLR4; MyD88; NF- $\kappa$ B(p65).

**Practical Application:** Pri could improve renal fibrosis by via regulation miRNA-145-5p to target TLR4.

## 1 Introduction

Renal interstitial fibrosis is a common pathway for the progression to end-stage renal disease. Due to various factors, there may be increased number of renal interstitial cells, enhanced synthesis of fibrin, inhibited degradation of matrix, and accumulation of extracellular matrix, which may seriously damage the renal cells and tissue structure, leading to the decline of renal function as well as fibrosis of renal tubules and glomerular fibrosis (Zeisberg & Neilson, 2010). The degree of renal interstitial fibrosis can objectively reflect the impairment of renal cells and renal function. Multiple signaling pathways are implicated in the pathogenesis of renal interstitial fibrosis, among which TLR4/MyD88/NF- $\kappa$ B(p65) signaling pathway has been explored comprehensively. Activation of this signaling pathway has been reported to be intimately associated with renal interstitial fibrosis and related inflammatory response (Mahmoud et al., 2019).

MicroRNAs (miRNAs) can regulate the expression of various proteins under physiological and pathological conditions (). MiRNAs are small noncoding RNA molecules containing 18-23 nucleotides that regulate protein levels through interactions with sequences in the 3'-untranslated region (3'-UTR) of target gene mRNA (Goto et al., 2016; Hou et al., 2016). MiR-145-5p belongs to miRNA family, which has been found to play an important role in inflammation and inflammation-induced organ damage (Gu et al., 2019; Zhang et al., 2019; Yan et al., 2019).

Pristimerin (Pri) is extracted primarily from the root bark of *Celastrus orbiculatus*. It has been found to have broad-spectrum anti-tumor, anti-inflammatory, antioxidant and other pharmacological activities (Deeb et al., 2014; Yan et al., 2013; Tiedemann et al., 2009; Byun et al., 2009; Wu et al., 2005). This study was carried out to investigate the effect of Pri on renal fibrosis by regulating miRNA-145-5p expression *in vivo* and *in vitro*, associated with the analysis of related mechanism. It is expected to provide experimental reference for the exploration of new therapeutic agents for the treatment of renal fibrosis.

## 2 Materials and methods

### 2.1 Experimental materials and animals

Pri, interleukin-1 $\beta$  (IL-1 $\beta$ ), superoxide dismutase (SOD), malondialdehyde (MDA) and tumor necrosis factor - $\alpha$  (TNF- $\alpha$ ) enzyme-linked immunosorbent assay (ELISA) kits (R&D, USA); Col-I, TLR4, MyD88, NF- $\kappa$ B(p65) and GAPDH antibodies (Abcam, UK); clean healthy male SD rats (180-200 g; Animal Center of Nanjing Medical University); human renal tubular epithelial cells (HK-2; ATCC); Masson staining and HE staining kits (Nanjing KeyGen Biotech Co., Ltd.); dual luciferase reporter gene assay kit (Promega); RNA extraction, reverse transcription and amplification kits (Takara, Dalian); si-NC (empty plasmid)

Received 12 Aug., 2021

Accepted 10 Sept., 2021

<sup>1</sup>Department of Nephrology, The First Affiliated Hospital of Wannan Medical College (Yijishan Hospital of Wannan Medical College), Wuhu, Anhui, China

\*Corresponding author: ahssxhh@163.com

and si-miRNA-145-5p (miRNA-145-5p inhibitor) (synthesized by Nanjing KeyGen Biotech Co., Ltd.).

## 2.2 Establishment of renal interstitial fibrosis model and grouping

45 SD rats were randomly divided into NC group, Model group, Pri-L group (1.0  $\mu\text{mol/kg}$ ), Pri-M group (2.0  $\mu\text{mol/kg}$ ) and Pri-H group (10.0  $\mu\text{mol/kg}$ ), with 9 rats in each group. All rats were fed adaptively for 1 week, and fasted 1 day before modeling, with free access to drinking. Using unilateral ureteral obstruction (UUO) to make renal interstitial fibrosis rat model. The rats were anesthetized by intraperitoneal injection of 10% chloral hydrate (4 mL/kg). After the successful anesthesia, the rats were fixed on the operating table (right lying position), with a routine skin preparation in the lower part of the left rib. The iodophor disinfectant (4.5 g/L) was used to sterilize three times in the operation area routinely, followed by the shopping of sterile hole sheet. The incision was made at the left costolumbar point, the skin was cut with sterile scalpel to separate subcutaneous tissue and muscular layer bluntly, and the peritoneum was cut until a clear exposure of the left renal tissue. The left renal artery and the left ureter were separated, and then the lower pole and calyces of the kidney were ligated with 7-0 silk thread. After that, the ureter in the middle part was cut off with sterile surgical scissors. Only left renal artery and left ureter were isolated in the control group. At the end of the operation, the abdominal cavity was washed with normal saline after kidney reduction, the incision was sutured layer by layer, and the incisional skin was applied with Iodophor and then pasted with sterile film. From the first day after operation, rats in the Model groups were given Pri at different dosages by gavage for 2 weeks. Rats in the NC group and Model group were provided the same volume of saline for 2 weeks.

## 2.3 Cell culture and grouping

HK-2 cells were cultured in DMEM low-glucose medium containing 10% fetal bovine serum at 37 °C with 5% CO<sub>2</sub>. The cells were subcultured when the cell density was about 80% under the microscope. The subcultured HK-2 cells were randomly divided into NC group, Model group (HK-2 cell were treated with 8 ng/ml TGF- $\beta$ 1 to make kidney fibrosis cell model), Pri group (10.0  $\mu\text{mol/L}$ ), Pri+si-NC (simultaneous treatment of HK-2 cells with Pri and transfection with si-NC) and Pri+si-miRNA (10.0  $\mu\text{mol/L}$  Pri treatment for HK-2 cells after cell transfection of si-miRNA-145-5p).

HK-2 which were logarithmic growth phase were stimulated by 10 ng/mL TGF- $\beta$ 1 to make renal interstitial fibrosis cell model.

HK-2 cells of the Model group, Pri group, Pri+si-NC group and Pri+si-miRNA group were treated with 10ng/mL TGF- $\beta$ 1.

## 2.4 Histopathological observation

HE staining and Masson staining were performed to observe the pathological changes of renal tissue. Eight non-overlapping high-power fields of vision ( $\times 200$ ) were randomly selected during the semi-quantitative analysis of Masson staining. Image Pro

Plus 6.0 was used to calculate the proportion of blue staining of the renal interstitium in the whole film to reflect the degree of renal fibrosis.

## 2.5 Renal function assessment

The levels of serum creatinine (Scr) and urea nitrogen (BUN) were measured by the Automatic Biochemical Tester.

## 2.6 ELISA assay

Blood samples were collected from the abdominal aorta of rats in each group after intragastric administration. Meanwhile, the supernatant of each group of cell culture medium was collected, centrifuged at 3,500 r/min for 15min to take the supernatant. TNF- $\alpha$ , IL-1 $\beta$ , MDA and SOD were determined according to the instructions of ELISA kit.

## 2.7 Detection of gene expression by RT-qPCR

After the total RNA was extracted from renal tissues and cells of each group, it was reverse transcribed into cDNA under the reaction conditions (37 °C for 15 min, 85 °C for 5 s, and 4 °C). Then, Real-time fluorescent quantitative PCR reaction was performed by using SYBR Green dye method. The reaction conditions were 95 °C for 30s; 95 °C for 5s, 60 °C for 34s, in a total of 40 cycles; followed by 95 °C for 15s, 60 °C for 60s, and 90 °C for 15s. U6 was selected as internal reference of miRNA-145-5p and GAPDH was the internal reference for other genes. The relative mRNA expression level of the target gene was calculated by 2<sup>- $\Delta\Delta\text{Ct}$</sup>  method. The primers were designed and synthesized by Sangon Biotech (Shanghai) Co., Ltd. and the primer sequence is shown in Table 1. The experiment was repeated 3 times in each group, with 3 replicates established.

## 2.8 Detection of protein expression by western blotting (WB)

An amount of 100 mg of renal tissue or HK-2 cells were taken for the extraction of the total protein in tissue or cells with tissue or cell lysate. It was separated by SDS-PAGE and transferred to PVDF membrane, followed by incubation with 5% skimmed milk powder at room temperature for 2 h. Subsequently, the

**Table 1.** Primer sequences for reverse transcription-quantitative PCR analysis.

Gene Name	Primer sequence
miRNA-145-5p	F: 5'-GTCCAGTTTCCCAGGAATCC-3' R: 5'-TCGCTTCGGCACATAT-3'
TLR4	F:5'-AAACTTGCCTTCAAACCTGGC-3' R:5'-ACCTGAACTCATCAATGGTCA-3'
MyD88	F:5'-ATAGGCACCAGCATGCAC-3' R: 5'-TAGGGTCCCTTACCAGGTA-3'
NF- $\kappa$ B(p65)	F:5'-TCACCAAAGACCCACCTCACC-3' R: 5'-CGCACCCGATTCAAGTCATAGT-3'
GAPDH	F:5'-ACAACCTTTGGTATCGTGGAAAG-3' R: 5'-GCCATCACGCCACAGTTTC-3'
U6	F:5'-CTCGCTTCGGCAGCAC-3' R: 5'-AACGCTTCACGAATTTGCGT-3'

primary antibody working solution was added and incubated overnight at 4 °C, and the secondary antibody working solution was supplemented and incubated at room temperature for 1 h after membrane washing with TBS-T buffer (×5, 10 min/time). After another membrane washing with TBS-T buffer (10 min/time), enhanced chemiluminescence (ECL) was used for development. The Gel Imaging System was used for photography and analysis.

### 2.9 Immunofluorescence detection of the translocation of NF-κB(p65) to the nucleus

The cells slides in each group were washed with PBS for three times and fixed with 4% paraformaldehyde for 10 min at room temperature. With PBS washing, cell slides were treated with 0.3% Triton-X100 at room temperature for 15min, washed with PBS again, and then sealed with 10% goat serum at room temperature for 30min. In the next step, rabbit anti-human NF-κB(p65) (1:100) was added and incubated at 4 °C overnight, and then the secondary antibody of anti-rabbit IgG H&L (1:500) was added and incubated at room temperature for 30 min after PBS washing. With another PBS washing, the cell slides were sealed with sealing liquid containing DAPI, which were observed and photographed under the fluorescence microscope. Image Pro Plus 6.0 software was used to measure the amount of protein transportation to the nucleus.

### 2.10 Double luciferase assay

MiRNA has been accepted as the most important post-transcriptional regulator of protein. The present study thus carried out a bioinformatics analysis of TLR4 targeting miRNA. All candidate genes meeting the criteria of targeting TLR4 mRNA and expressing in kidney were screened. Targetscan algorithm was used to predict the candidate miRNA target of TLR4, and luciferase reporter gene was constructed by molecular cloning technology. TLR4 3'-UTR target sequence and TLR4 3'-UTR(TLR4 3'-UTR Mul) with mutation at the binding site of miRNA-145-5p were all purchased from Creative Biogene (Shirley, NY, USA).

### 2.11 Statistical analysis

Statistical analysis of this study was performed by using SPSS 20.0 statistical software. The measurement data were expressed by Mean ± Standard Deviation (Mean ± SD) and compared by using the variance of analysis, and further pair-wise comparison was made by One Way ANOVA assay.  $P < 0.05$  meant that the difference was statistically significant.

## 3 Results

### 3.1 Renal histopathological changes of rats in each group

According to the results of HE staining, the structure of glomeruli and renal tubules in NC group was clearly displayed, with no inflammatory cell infiltration in the renal interstitium, no fibrous tissue proliferation, no mesangial cell or stromal tissue proliferation. In Model group, there were glomerular stromal tissue hyperplasia, Bowman's capsule expansion, renal tubular

epithelial cell swelling and vacuolar degeneration, focal necrosis, patchy atrophy, and even epithelial cell necrosis and abscission in renal tubular lumen. Besides, there were diffuse infiltration of renal interstitial inflammatory cells, proliferation of fibrous tissue and even patchy fibrosis change. After Pri intervention at different dosages, there were decreased infiltration of inflammatory cells, more regular arrangement of renal tubules and smaller size of interstitial fibrosis area (Figure 1A). The results of Masson staining showed that the ratio of area stained using Masson's trichrom stain in Model group was significantly higher than that in NC group ( $P < 0.001$ , Figure 1B). compared with the Model group, the ratio of area stained using Masson's trichrom stain in Pri intervention groups was significantly inhibited after Pri intervention ( $P < 0.05$ , respectively, Figure 1B). Besides, there were statistically significant differences among all Pri intervention groups ( $P < 0.05$ , respectively, Figure 1B).

### 3.2 Effect of Pri on Scr and BUN in rats with renal interstitial fibrosis

As shown in Figure 2, there was a significant difference in the levels of Scr and BUN in each group ( $P < 0.05$ ). Further pair-wise comparison showed that the level of Scr and BUN in the Model group was higher than that in the NC group ( $P < 0.05$ ). Compared with the Model group, the levels of Scr and BUN in Pri intervention groups decreased in a dose-dependent manner ( $P < 0.05$ ).

### 3.3 Effect of Pri on serum IL-1β, TNF-α, SOD and MDA contents in rats with renal interstitial fibrosis

Statistically significant difference was observed in the comparison of serum IL-1β, TNF-α, SOD and MDA contents in rats among groups ( $P < 0.05$ ). Further pair-wise comparison revealed that there were increase in the content of IL-1β, TNF-α and MDA, but decrease in the content of SOD when compared the Model group with the NC group ( $P < 0.001$ ). After Pri intervention, compared with the Model group, serum IL-1β, TNF-α and MDA contents decreased in a dose-dependent manner, while serum SOD content increased in a dose-dependent manner in Pri intervention groups ( $P < 0.05$ ). Detailed statistical analysis results are shown in Figure 3.

### 3.4 Effect of Pri on related gene expressions in renal tissue

In view of the detection results of RT-qPCR (Figure 4), compared with the NC group, there were increase in the mRNA expression of TLR4, MyD88 and NF-κB(p65), but decrease in the mRNA expression of miRNA-145-5p in Model group ( $P < 0.001$ ). After Pri intervention, compared with the Model group, the mRNA expression of TLR4, MyD88 and NF-κB(p65) decreased while that of SOD increased in a dose-dependent manner in Pri intervention groups ( $P < 0.05$ ).

### 3.5 Effect of Pri on related protein expressions in renal tissue

WB detection results (Figure 5) revealed that compared with the NC group, the protein expression of TLR4, MyD88 and NF-κB(p65) were increased in Model group ( $P < 0.001$ ).

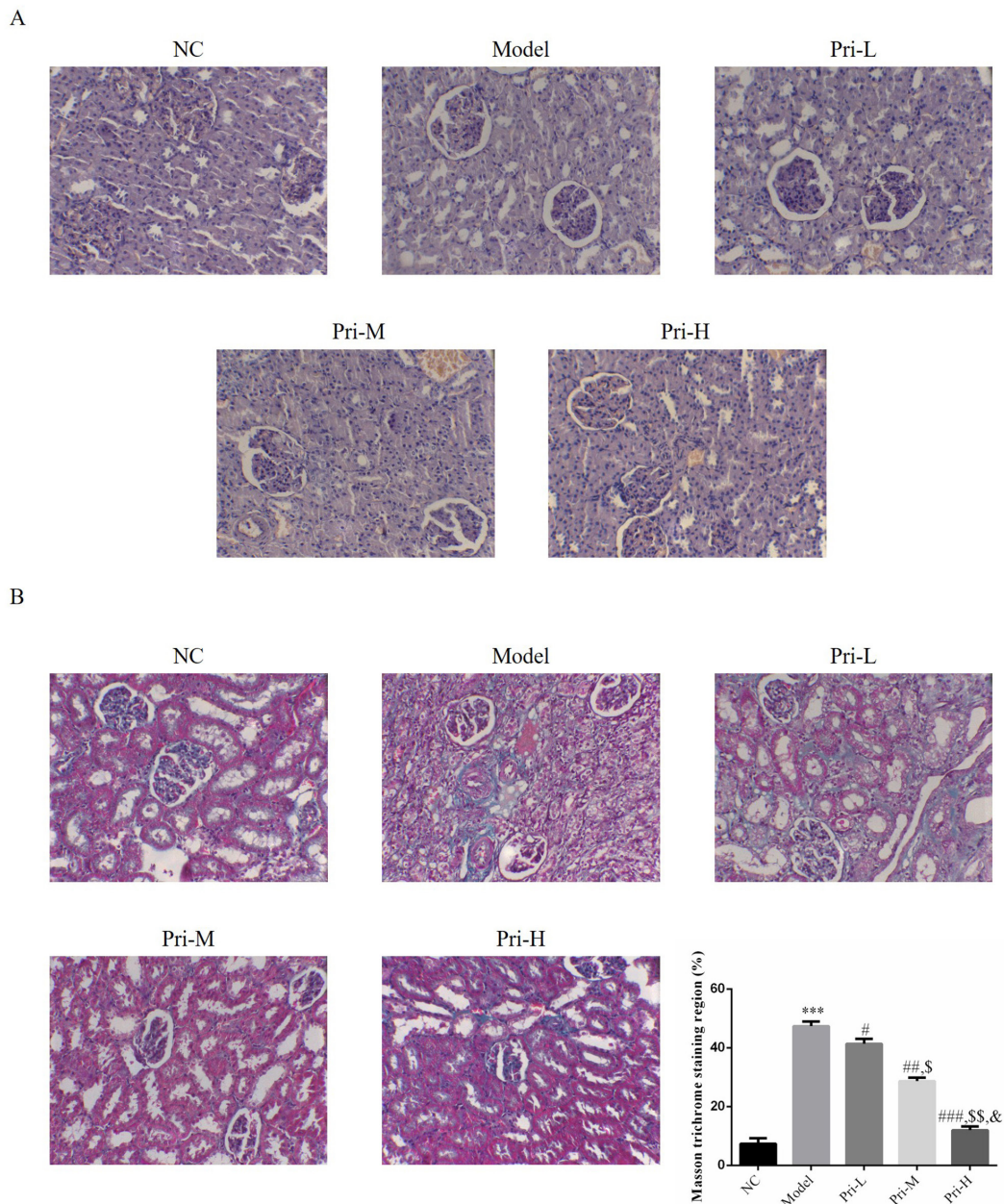


**Figure 1.** The pathological and fibrosis levels by HE and Masson staining. NC: The rats were treated with normal; Model: UUO model rats; Pri-L: UUO model rats were treated with 1.0  $\mu\text{mol/kg}$  Pri; Pri-M: UUO model rats were treated with 2.0  $\mu\text{mol/kg}$  Pri; Pri-H: UUO model rats were treated with 10.0  $\mu\text{mol/kg}$  Pri. (A) The pathological of difference rats by HE staining (200 $\times$ ); (B) Masson trichrome staining region of difference rats groups by Masson staining (200 $\times$ ). \*\*\*:  $P < 0.001$ , compared with NC group; #:  $P < 0.05$ , ##:  $P < 0.01$ , ###:  $P < 0.001$ , compared with Model group; \$:  $P < 0.05$ , \$\$:  $P < 0.01$ , compared with Pri-L; &:  $P < 0.05$ , compared with Pri-M.

Following intervention with Pri, compared with the Model group, the protein expression of TLR4, MyD88 and NF- $\kappa\text{B}$ (p65) decreased in a dose-dependent manner in Pri intervention groups ( $P < 0.05$ ).

### 3.6 Effect of miRNA-145-5p on the content of IL-1 $\beta$ , TNF- $\alpha$ , SOD and MDA

Compared with the NC group, there was significant increase in the content of IL-1 $\beta$ , TNF- $\alpha$  and MDA but decrease in that of

SOD in the Model group ( $P < 0.001$ ). Furthermore, compared with the Model group, Pri group and Pri+si-NC group showed significant decrease in the content of IL-1 $\beta$ , TNF- $\alpha$  and MDA but increase in that of SOD ( $P < 0.001$ ). However, following the transfection of si-miRNA-145-5p into HK-2 cells, there were obvious increase in the content of IL-1 $\beta$ , TNF- $\alpha$  and MDA but decrease in that of SOD in the Pri+si-miRNA group when compared with that of the Pri group ( $P < 0.001$ ). Corresponding results are displayed in Figure 6.

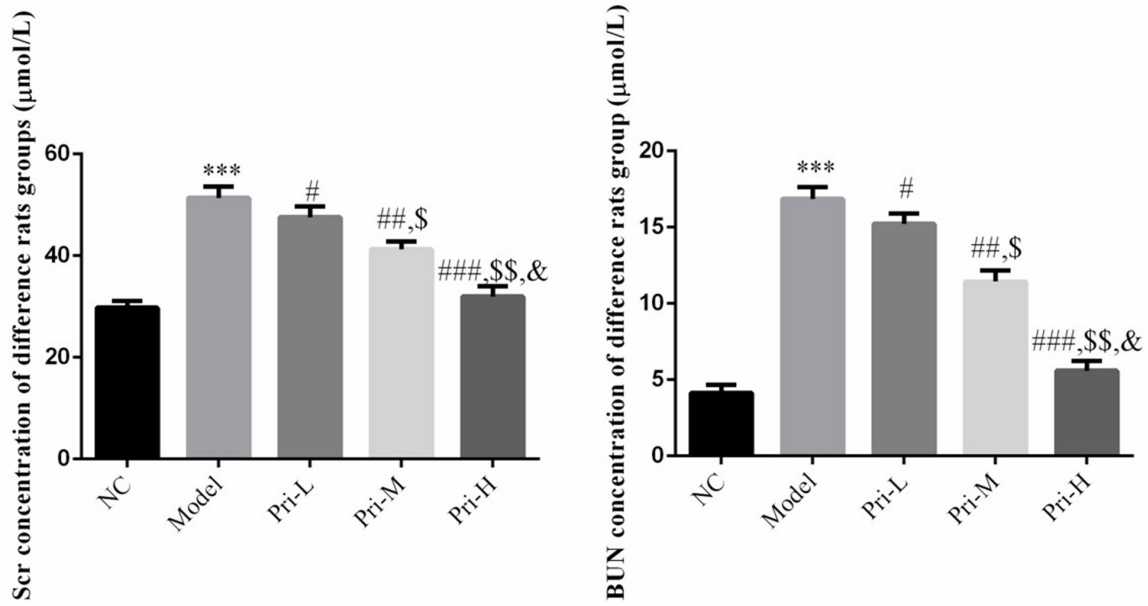


**Figure 2.** Scr and BUN concentrations of difference rats groups in serum. NC: The rats were treated with normal; Model: UUU model rats; Pri-L: UUU model rats were treated with 1.0 µmol/kg Pri; Pri-M: UUU model rats were treated with 2.0 µmol/kg Pri; Pri-H: UUU model rats were treated with 10.0 µmol/kg Pri. \*\*\*:  $P < 0.001$ , compared with NC group; #:  $P < 0.05$ , #:  $P < 0.01$ , ###:  $P < 0.001$ , compared with Model group; \$:  $P < 0.05$ , \$\$:  $P < 0.01$ , compared with Pri-L; &:  $P < 0.05$ , compared with Pri-M.

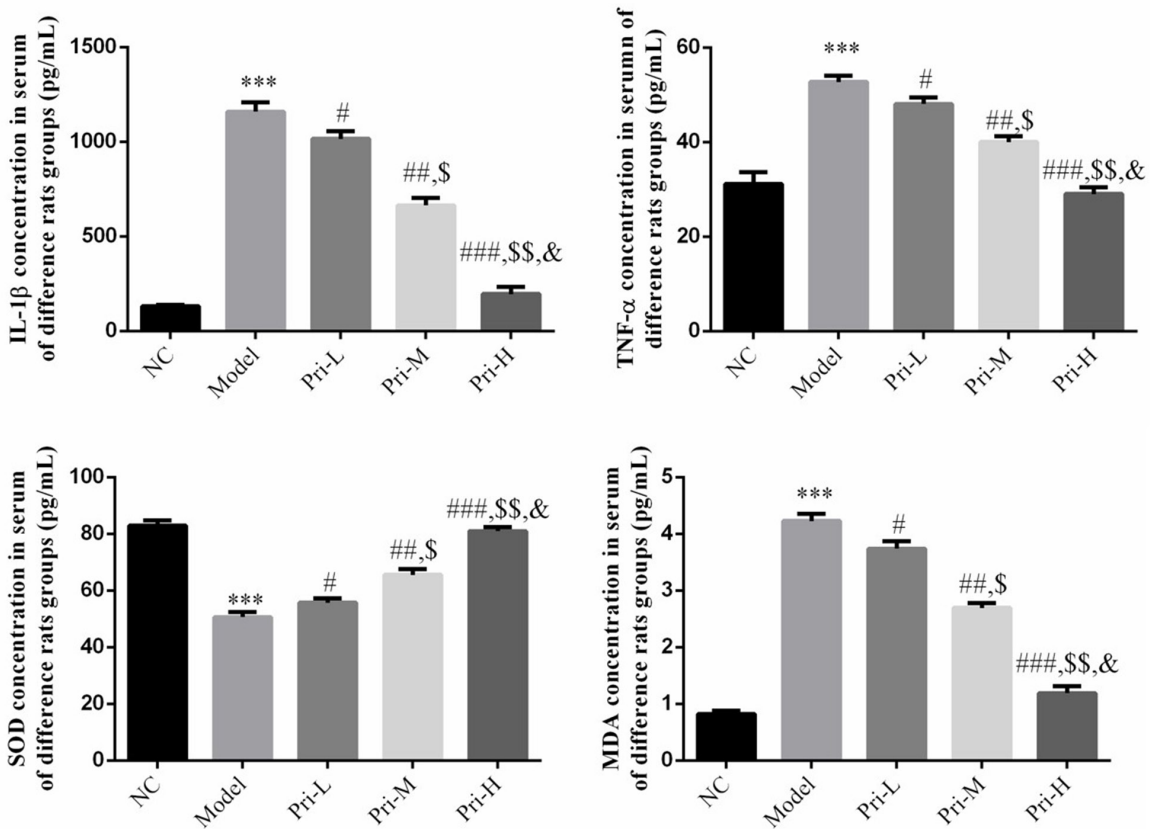


**Figure 3.** IL-1 $\beta$ , TNF- $\alpha$ , SOD and MDA concentrations of difference rats groups in serum. NC: The rats were treated with normal; Model: UUU model rats; Pri-L: UUU model rats were treated with 1.0 µmol/kg Pri; Pri-M: UUU model rats were treated with 2.0 µmol/kg Pri; Pri-H: UUU model rats were treated with 10.0 µmol/kg Pri. \*\*\*:  $P < 0.001$ , compared with NC group; #:  $P < 0.05$ , #:  $P < 0.01$ , ###:  $P < 0.001$ , compared with Model group; \$:  $P < 0.05$ , \$\$:  $P < 0.01$ , compared with Pri-L; &:  $P < 0.05$ , compared with Pri-M.

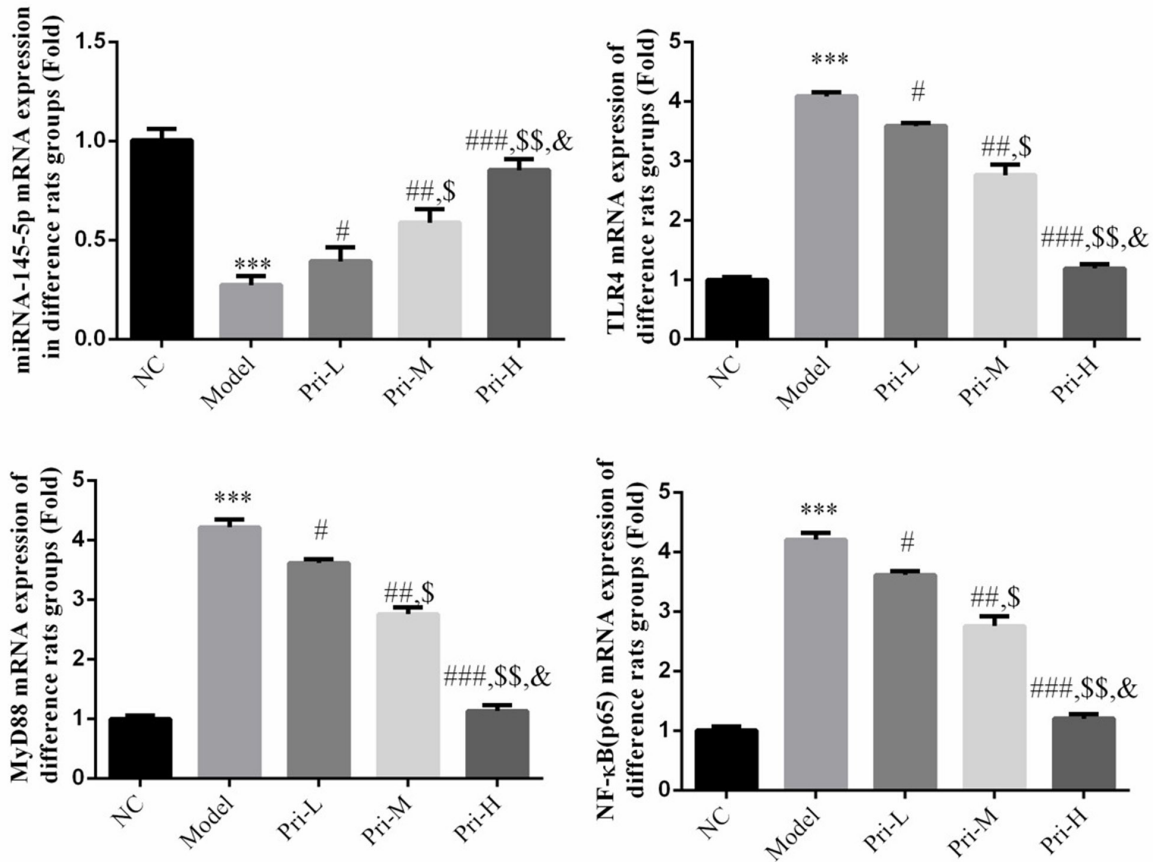


**Figure 4.** Relative gene expressions in difference rats groups in kidney tissues by RT-qPCR assay. NC: The rats were treated with normal; Model: UUU model rats; Pri-L: UUU model rats were treated with 1.0 $\mu$ mol/kg Pri; Pri-M: UUU model rats were treated with 2.0 $\mu$ mol/kg Pri; Pri-H: UUU model rats were treated with 10.0  $\mu$ mol/kg Pri. \*\*\*:  $P < 0.001$ , compared with NC group; #:  $P < 0.05$ , ##:  $P < 0.01$ , ###:  $P < 0.001$ , compared with Model group; \$:  $P < 0.05$ , \$\$:  $P < 0.01$ , compared with Pri-L; &:  $P < 0.05$ , compared with Pri-M.

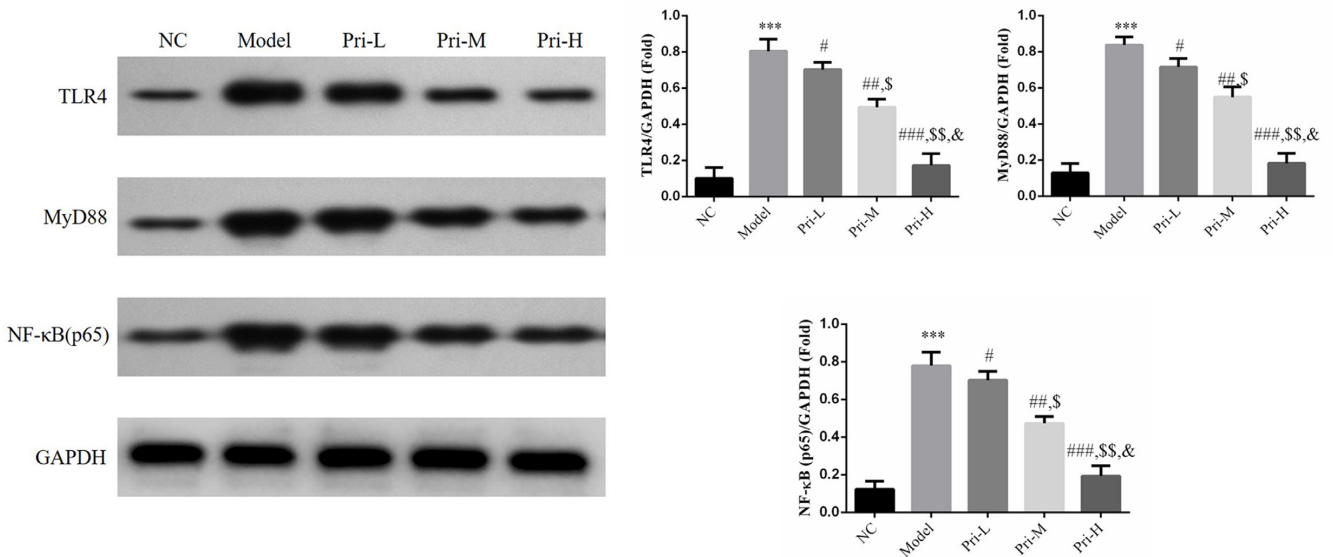


**Figure 5.** Relative proteins expression by WB assay in difference rats groups. NC: The rats were treated with normal; Model: UUU model rats; Pri-L: UUU model rats were treated with 1.0  $\mu$ mol/kg Pri; Pri-M: UUU model rats were treated with 2.0  $\mu$ mol/kg Pri; Pri-H: UUU model rats were treated with 10.0  $\mu$ mol/kg Pri. \*\*\*:  $P < 0.001$ , compared with NC group; #:  $P < 0.05$ , ##:  $P < 0.01$ , ###:  $P < 0.001$ , compared with Model group; \$:  $P < 0.05$ , \$\$:  $P < 0.01$ , compared with Pri-L; &:  $P < 0.05$ , compared with Pri-M.

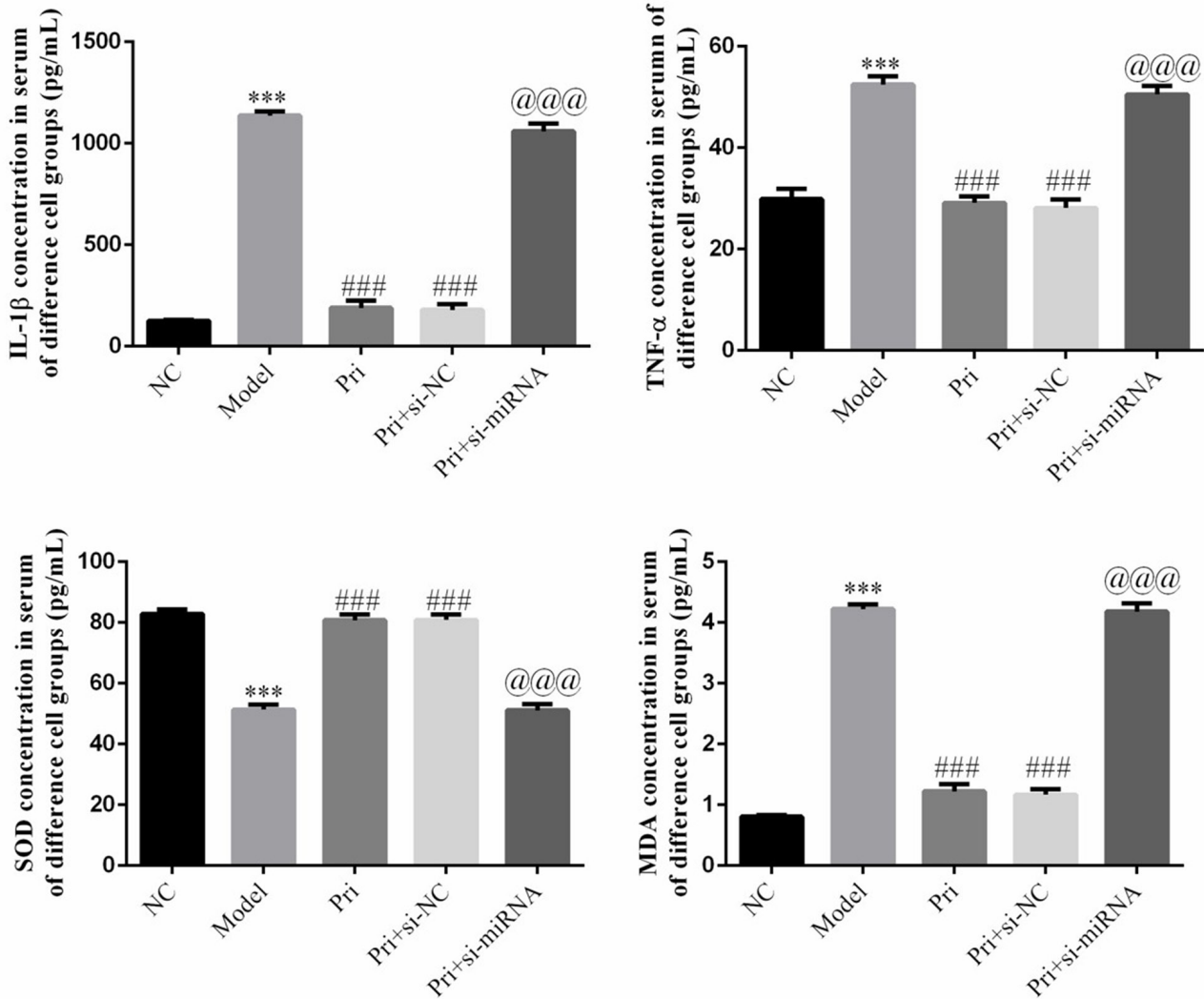


**Figure 6.** IL-1 $\beta$ , TNF- $\alpha$ , SOD and MDA concentrations of difference cell groups in supernatant. NC: HK-2 cell were treated with normal; Model: HK-2 treated with 10ng/mL TGF- $\beta$ 1; Pri: HK-2 treated with 10 ng/mL TGF- $\beta$ 1 and 10.0  $\mu$ mol/kg Pri; Pri+si-NC: HK-2 treated with 10 ng/mL TGF- $\beta$ 1, transfected with si-NC(negative control) and treated with 10.0  $\mu$ mol/kg Pri; Pri+si-miRNA: HK-2 treated with 10 ng/mL TGF- $\beta$ 1, transfected with si-miRNA-145-5p(inhibiting miRNA-145-5p expression) and treated with 10.0  $\mu$ mol/kg Pri. \*\*\*:  $P < 0.001$ , compared with NC; ###:  $P < 0.001$ , compared with Model group; @@@:  $P < 0.001$ , compared with Pri group.

### 3.7 Gene expression levels in different groups after cell transfection

There were significant decrease in miRNA-145-5p expression level, but evident increase in TLR4, MyD88 and NF- $\kappa$ B(p65) mRNA expression levels in the Model group when compared to those in the NC group ( $P < 0.001$ ). With Pri intervention, compared with the Model group, significant upregulation in miRNA-145-5p expression was found in the Pri group and Pri+si-NC group, while the mRNA expression levels of TLR4, MyD88 and NF- $\kappa$ B(p65) were obviously downregulated ( $P < 0.001$ ). When miRNA-145-5p inhibitor, i.e., si-miRNA-145-5p, was transfected into cells, the therapeutic effect of Pri was reversed. Specifically, compared with the Pri group, the aforementioned transfection resulted in significant decrease in miRNA-145-5p expression, but obvious increase in the mRNA expression levels

of TLR4, MyD88 and NF- $\kappa$ B(p65) ( $P < 0.001$ ), relative data were shown in Figure 7.

### 3.8 Protein expression levels in different groups after cell transfection

As shown in Figure 8, compared with the NC group, TLR4, MyD88 and NF- $\kappa$ B(p65) protein expression levels were significantly increased in the Model group ( $P < 0.001$ ). After Pri intervention, there were remarkable increase in the protein expression levels of TLR4, MyD88 and NF- $\kappa$ B(p65) in the Pri group and Pri+si-NC group when compared to those of the Model group ( $P < 0.001$ ). The therapeutic effect of Pri was reversed after cell transfection of miRNA-145-5p inhibitor (si-miRNA-145-5p), resulting in significant increase in the protein expression

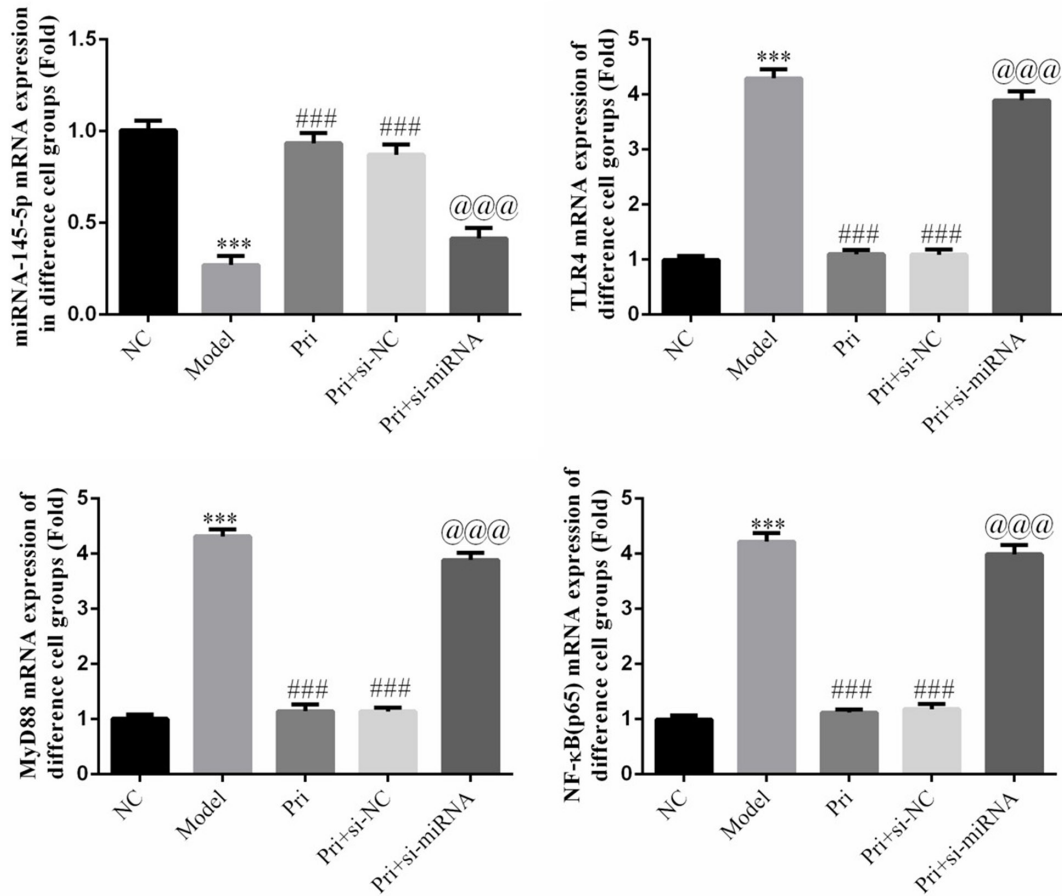


**Figure 7.** Relative gene expressions in difference cell groups by RT-qPCR assay. NC: HK-2 cell were treated with normal; Model: HK-2 treated with 10ng/mL TGF- $\beta$ 1; Pri: HK-2 treated with 10 ng/mL TGF- $\beta$ 1 and 10.0  $\mu$ mol/kg Pri; Pri+si-NC: HK-2 treated with 10 ng/mL TGF- $\beta$ 1, transfected with si-NC(negative control) and treated with 10.0  $\mu$ mol/kg Pri; Pri+si-miRNA: HK-2 treated with 10 ng/mL TGF- $\beta$ 1, transfected with si-miRNA-145-5p(inhibiting miRNA-145-5p expression) and treated with 10.0  $\mu$ mol/kg Pri. \*\*\*:  $P < 0.001$ , compared with NC; ###:  $P < 0.001$ , compared with Model group; @@@:  $P < 0.001$ , compared with Pri group

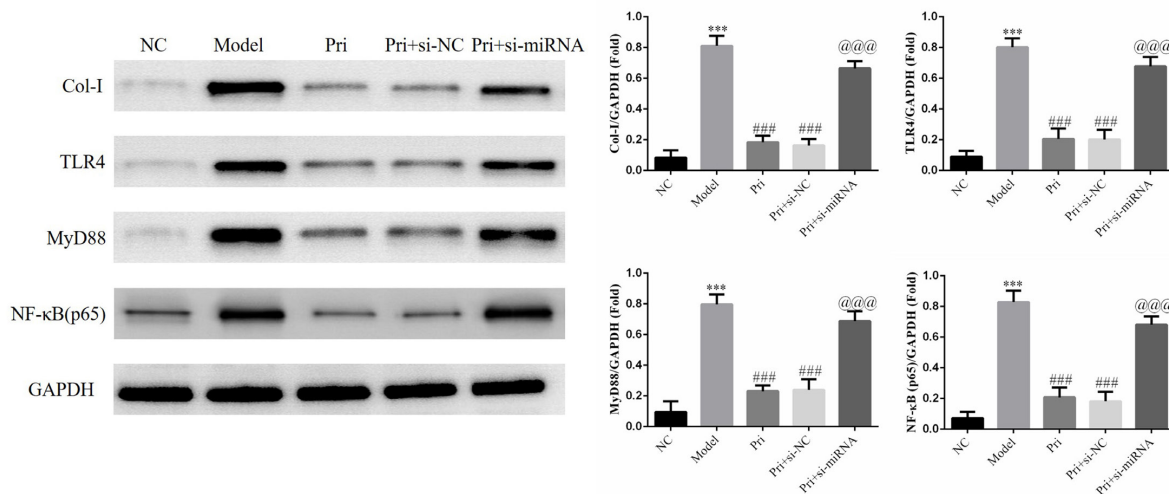


**Figure 8.** Relative proteins expressions by WB assay. NC: HK-2 cell were treated with normal; Model: HK-2 treated with 10 ng/mL TGF- $\beta$ 1; Pri: HK-2 treated with 10ng/mL TGF- $\beta$ 1 and 10.0  $\mu$ mol/kg Pri; Pri+si-NC: HK-2 treated with 10 ng/mL TGF- $\beta$ 1, transfected with si-NC (negative control) and treated with 10.0  $\mu$ mol/kg Pri; Pri+si-miRNA: HK-2 treated with 10ng/mL TGF- $\beta$ 1, transfected with si-miRNA-145-5p (inhibiting miRNA-145-5p expression) and treated with 10.0 $\mu$ mol/kg Pri. \*\*\*:  $P < 0.001$ , compared with NC; ###:  $P < 0.001$ , compared with Model group; @@@:  $P < 0.001$ , compared with Pri group.

levels of TLR4, MyD88 and NF-κB(p65) when compared with the Pri group ( $P < 0.001$ ).

### 3.9 Detection of the translocation of NF-κB(p65) to the nucleus in different groups after cell transfection

Compared with the NC group, the quantity of the translocation of NF-κB(p65) to the nucleus was significantly increased in the Model group ( $P < 0.001$ ). With Pri intervention, it was obviously decreased in the Pri group and Pri+si-NC group than that in the Model group ( $P < 0.001$ ). Moreover, the effect of Pri was reversed after cell transfection of miRNA-145-5p inhibitor (si-miRNA-145-5p), and the quantity of translocation of NF-κB(p65)

to the nucleus obviously increased when compared to that in the Pri group ( $P < 0.001$ ). The results are described in Figure 9.

### 3.10 Target relationship analysis of miRNA-145-5p and TLR4 dual luciferase reporter gene assay

According to the results of dual luciferase reporter gene assay, in TLR4-Mul (TLR4 mutant type), there was no significant difference in fluorescence intensity between miRNA-NC group and miRNA-145-5p group. By contrast, in TLR4-WT (TLR4 wild type), the fluorescence intensity was significantly inhibited in the miRNA-145-5p group ( $P < 0.001$ , Figure 10). The results suggested that miRNA-145-5p could target TLR4 in HK-2 cells.

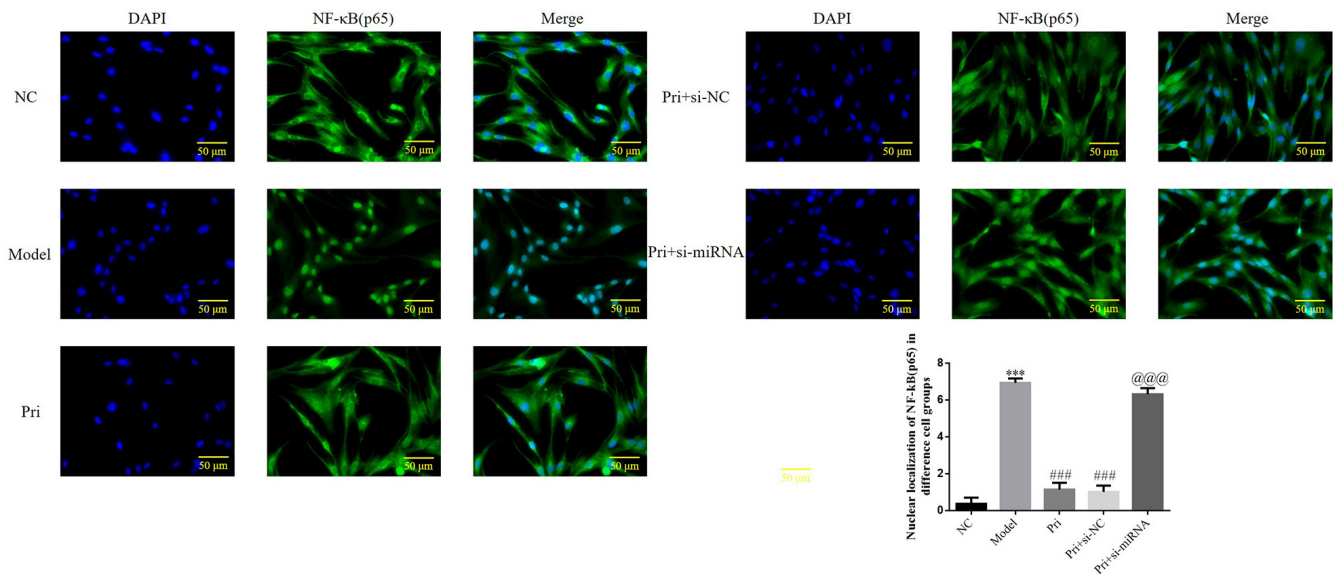


**Figure 9.** NF-κB(p65) nuclear volume of difference groups. NC: HK-2 cell were treated with normal; Model: HK-2 treated with 10 ng/mL TGF-β1; Pri: HK-2 treated with 10 ng/mL TGF-β1 and 10.0 μmol/kg Pri; Pri+si-NC: HK-2 treated with 10 ng/mL TGF-β1, transfected with si-NC(negative control) and treated with 10.0 μmol/kg Pri; Pri+si-miRNA: HK-2 treated with 10ng/mL TGF-β1, transfected with si-miRNA-145-5p(inhibiting miRNA-145-5p expression) and treated with 10.0 μmol/kg Pri. \*\*\*:  $P < 0.001$ , compared with NC; ###:  $P < 0.001$ , compared with Model group; @@@:  $P < 0.001$ , compared with Pri group.

	Predicted consequential pairing of target region (top) and miRNA (bottom)	Site type	Context++ score	Context++ score percentile	Weighted context++ score	Conserved branch length	PCT
Position 6682-6688 of TLR4 3' UTR	5' ... UGAGAGCAUGGAUGGAACUGGAG ...	7mer-m8	-0.02	47	0.00	0.241	< 0.1
hsa-miR-145-5p	3' UCCCUAAGGACCCUUUGACCUG						

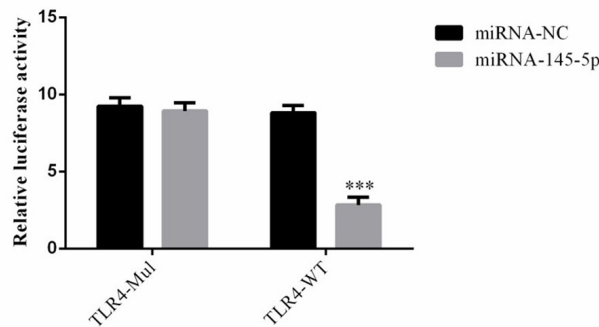


**Figure 10.** Double luciferase assay. miRNA-NC: cell were transfected with miRNA-NC (negative control); miRNA-145-5p: cell were transfected with miRNA-145-5p. \*\*\*:  $P < 0.001$ , compared with miRNA-NC.

## 4 Discussion

The development of renal interstitial fibrosis may be attributed to the involvement of multiple cellular events, multiple molecules, as well as multiple signal transduction pathways regulation and interaction. It is primarily characterized by proliferation of renal interstitial fibroblasts, excessive accumulation of extracellular matrix and mesenchymal transdifferentiation of renal tubular epithelial cells from the perspective of pathology (Kanasaki, et al., 2013), among which the first and the third events constitute the main factors of renal interstitial fibrosis. In this study, according to the HE staining, Masson staining and ELISA results, rats with renal interstitial fibrosis rats showed glomerular stromal tissue hyperplasia, Bowman's capsule expansion, renal tubular epithelial cell swelling and vacuolar degeneration, focal necrosis, patchy atrophy, epithelial cell necrosis and abscission in renal tubular lumen, diffuse infiltration of renal interstitial inflammatory cells, as well as patchy fibrosis change. The renal tubular epithelial cells and renal interstitium of the control group and the normal rats with gavage were observed to be roughly normal by histopathology. The above morphological findings were consistent with relevant literature (Liu, et al., 2014), indicating the feasibility and success of the establishment of animal model adopted in this experiment. After 2 weeks of gavage administration of Pri, there were improvement in the infiltration of inflammatory cells and the swelling degree of renal tubular epithelial cells, accompanied by reduced area of interstitial fibrosis. The structure of renal tubules was clear and there was no denatured and necrotic cells in the lumen based on the histological staining. In addition, epithelial cells on the tube wall were arranged regularly without atrophy, with the observation of clear renal interstitial structure and no fibrosis as well. At the same time, our study also supported that the anti-renal interstitial fibrosis role of Pri manifested in renal tubular epithelial cells primarily.

Scr and BUN are commonly used markers of renal function, both of which are excreted by kidney. Creatinine is produced in muscle metabolism as the end-product of creatine phosphate. In this study, it was found that Scr and BUN content increased in the Model group, but decreased after gavage administration of Pri at different concentrations, suggesting that Pri could improve renal interstitial fibrosis. Simultaneously, Pri intervention resulted in the increased activity of SOD and inhibited content of MDA and inflammatory factors (IL-1 $\beta$  and TNF- $\alpha$ ). Meanwhile, RT-qPCR showed that the gene expression of miRNA-145-5p was significantly inhibited by Pri intervention.

It has been recognized that miRNA regulates specific target gene expression by inhibiting gene transcription or silencing corresponding mRNA, which exerts a regulatory role in cell activation, proliferation and apoptosis. Abnormal expression of miRNA may lead to damage of cell function, renal fibrosis, tumor and diabetes. Accumulated evidence supports that some specific miRNAs can regulate the occurrence and development of renal fibrosis through multiple channels (Chandrasekaran et al., 2012; Trionfini et al., 2015; Wang et al., 2013). In this study, luciferase activity analysis verified that miRNA-145-5p can regulate TLR4 targetedly. Pri can effectively improve the expression of miRNA-145-5p in renal fibrosis cells and animal model, then inhibit the

expression of TLR4 targetedly, and eventually improved the pathological changes of renal fibrosis.

In view of the important mechanism of the occurrence of renal fibrosis, it is speculated that MyD88 may be activated after the activation of TLR4, which subsequently induce the downstream translocation of NF- $\kappa$ B(p65) to the nucleus, and finally cause the release of various inflammatory cytokines (TNF- $\alpha$ , IL-6 and IL-1 $\beta$ ). The mechanism of pro-inflammatory cytokines promoting renal fibrosis lies in that highly expressed IL-1 $\beta$  is the key factor to promote renal fibrosis (Li et al., 2019; Sierra-Mondragon et al., 2018; Zhou et al., 2017). The findings of this study revealed that Pri could effectively inhibit TLR4/MyD88 expression, and then reduce the quantity of the translocation of NF- $\kappa$ B(p65) to the nucleus, which may be explained primarily by the increase of miRNA-145-5p expression.

In conclusion, both *in vitro* and *in vivo* experiments in our study support that Pri has a positive role in improving renal fibrosis by upregulating miRNA-145-5p expression, inhibit TLR4/MyD88 protein expression, and then decrease the translocation of NF- $\kappa$ B(p65) to the nucleus.

## Ethical approval

This study was approved by ethical approval of First Affiliated Hospital of Wannan Medical College(Yijishan Hospital of Wannan Medical College) (No.20190816-2).

## Conflict of interest

There were no conflict of interest in our study.

## Author contributions

Chen Xiao-Mei and Xu Hai-Hong design the experimental scheme; Chen Xiao-Mei,Zhang Jin-Yu,Yang Yan-Lang,Wang Yu-Wei and Yu Yuan-Yuan finished whole experiments in our study; Xu Hai-Hong checked whole data and grammar of manuscript; Chen Xiao-Mei written the manuscript.

## References

- Byun, J. Y., Kim, M. J., Eum, D. Y., Yoon, C. H., Seo, W. D., Park, K. H., Hyun, J. W., Lee, Y. S., Lee, J. S., Yoon, M. Y., & Lee, S. J. (2009). Reactive oxygen species-dependent activation of Bax and poly(ADP-ribose) polymerase-1 is required for mitochondrial cell death induced by triterpenoid pristimerin in human cervical cancer cells. *Molecular Pharmacology*, 76(4), 734-744. <http://dx.doi.org/10.1124/mol.109.056259>. PMID:19574249.
- Chandrasekaran, K., Karolina, D. S., Sepramaniam, S., Armugam, A., Marelyn Wintour, E., Bertram, J. F., & Jeyaseelan, K. (2012). Role of microRNAs in kidney homeostasis and disease. *Kidney International*, 81(7), 617-627. <http://dx.doi.org/10.1038/ki.2011.448>. PMID:22237749.
- Deeb, D., Gao, X., Liu, Y. B., Pindolia, K., & Gautam, S. C. (2014). Pristimerin, a quinonemethide triterpenoid, induces apoptosis in pancreatic cancer cells through the inhibition of pro-survival Akt/NF- $\kappa$ B/mTOR signaling proteins and anti-apoptotic Bcl-2. *International Journal of Oncology*, 44(5), 1707-1715. <http://dx.doi.org/10.3892/ijo.2014.2325>. PMID:24603988.
- Goto, Y., Kurozumi, A., Nohata, N., Kojima, S., Matsushita, R., Yoshino, H., Yamazaki, K., Ishida, Y., Ichikawa, T., Naya, Y., & Seki, N. (2016).

- The microRNA signature of patients with sunitinib failure: regulation of UHRF1 pathways by microRNA-101 in renal cell carcinoma. *Oncotarget*, 7(37), 59070-59086. <http://dx.doi.org/10.18632/oncotarget.10887>. PMID:27487138.
- Gu, W., Yuan, Y., Wang, L., Yang, H., Li, S., Tang, Z., & Li, Q. (2019). Long non-coding RNA TUG1 promotes airway remodelling by suppressing the miR-145-5p/DUSP6 axis in cigarette smoke-induced COPD. *Journal of Cellular and Molecular Medicine*, 23(11), 7200-7209. <http://dx.doi.org/10.1111/jcmm.14389>. PMID:31557398.
- Hou, X., Tian, J., Geng, J., Li, X., Tang, X., Zhang, J., & Bai, X. (2016). MicroRNA-27a promotes renal tubulointerstitial fibrosis via suppressing PPAR $\gamma$  pathway in diabetic nephropathy. *Oncotarget*, 7(30), 47760-47776. <http://dx.doi.org/10.18632/oncotarget.10283>. PMID:27351287.
- Kanasaki, K., Taduri, G., & Koya, D. (2013). Diabetic nephropathy: the role of inflammation in fibroblast activation and kidney fibrosis. *Frontiers in endocrinology*, 4, 7. <http://dx.doi.org/10.3389/fendo.2013.00007>. PMID:23390421.
- Li, R., Guo, Y., Zhang, Y., Zhang, X., Zhu, L., & Yan, T. (2019). Salidroside Ameliorates Renal Interstitial Fibrosis by Inhibiting the TLR4/NF- $\kappa$ B and MAPK Signaling Pathways. *International Journal of Molecular Sciences*, 20(5), E1103. <http://dx.doi.org/10.3390/ijms20051103>. PMID:30836660.
- Liu, C. F., Liu, H., Fang, Y., Jiang, S. H., Zhu, J. M., & Ding, X. Q. (2014). Rapamycin reduces renal hypoxia, interstitial inflammation and fibrosis in a rat model of unilateral ureteral obstruction. *Clinical and Investigative Medicine. Medecine Clinique et Experimentale*, 37(3), E142. <http://dx.doi.org/10.25011/cim.v37i3.21381>. PMID:24895989.
- Mahmoud, A. M., Desouky, E. M., Hozayen, W. G., Bin-Jumah, M., El-Nahass, E. S., Soliman, H. A., & Farghali, A. A. (2019). Mesoporous silica nanoparticles trigger liver and kidney injury and fibrosis via altering TLR4/NF- $\kappa$ B, JAK2/STAT3 and Nrf2/HO-1 signaling in rats. *Biomolecules*, 9(10), E528. <http://dx.doi.org/10.3390/biom9100528>. PMID:31557909.
- Sierra-Mondragon, E., Molina-Jijon, E., Namorado-Tonix, C., Rodríguez-Muñoz, R., Pedraza-Chaverri, J., & Reyes, J. L. (2018). All-trans retinoic acid ameliorates inflammatory response mediated by TLR4/NF- $\kappa$ B during initiation of diabetic nephropathy. *The Journal of Nutritional Biochemistry*, 60, 47-60. <http://dx.doi.org/10.1016/j.jnutbio.2018.06.002>. PMID:30193155.
- Tiedemann, R. E., Schmidt, J., Keats, J. J., Shi, C. X., Zhu, Y. X., Palmer, S. E., Mao, X., Schimmer, A. D., & Stewart, A. K. (2009). Identification of a potent natural triterpenoid inhibitor of proteasome chymotrypsin-like activity and NF-kappaB with antimyeloma activity in vitro and in vivo. *Blood*, 113(17), 4027-4037. <http://dx.doi.org/10.1182/blood-2008-09-179796>. PMID:19096011.
- Trionfini, P., Benigni, A., & Remuzzi, G. (2015). MicroRNAs in kidney physiology and disease. *Nature Reviews. Nephrology*, 11(1), 23-33. <http://dx.doi.org/10.1038/nrneph.2014.202>. PMID:25385286.
- Wang, J., Gao, Y., Ma, M., Li, M., Zou, D., Yang, J., Zhu, Z., & Zhao, X. (2013). Effect of miR-21 on renal fibrosis by regulating MMP-9 and TIMP1 in kk-ay diabetic nephropathy mice. *Cell Biochemistry and Biophysics*, 67(2), 537-546. <http://dx.doi.org/10.1007/s12013-013-9539-2>. PMID:23443810.
- Wu, C. C., Chan, M. L., Chen, W. Y., Tsai, C. Y., Chang, F. R., & Wu, Y. C. (2005). Pristimerin induces caspase-dependent apoptosis in MDA-MB-231 cells via direct effects on mitochondria. *Molecular Cancer Therapeutics*, 4(8), 1277-1285. <http://dx.doi.org/10.1158/1535-7163.MCT-05-0027>. PMID:16093444.
- Yan, J. J., Qiao, M., Li, R. H., Zhao, X. T., Wang, X. Y., & Sun, Q. (2019). Downregulation of miR-145-5p contributes to hyperproliferation of keratinocytes and skin inflammation in psoriasis. *The British Journal of Dermatology*, 180(2), 365-372. <http://dx.doi.org/10.1111/bjd.17256>. PMID:30269330.
- Yan, Y. Y., Bai, J. P., Xie, Y., Yu, J. Z., & Ma, C. G. (2013). The triterpenoid pristimerin induces U87 glioma cell apoptosis through reactive oxygen species-mediated mitochondrial dysfunction. *Oncology Letters*, 5(1), 242-248. <http://dx.doi.org/10.3892/ol.2012.982>. PMID:23255929.
- Zeisberg, M., & Neilson, E. G. (2010). Mechanisms of tubulointerstitial fibrosis. *Journal of the American Society of Nephrology*, 21(11), 1819-1834. <http://dx.doi.org/10.1681/ASN.2010080793>. PMID:20864689.
- Zhang, J., Cui, C., & Xu, H. (2019). Downregulation of miR-145-5p elevates retinal ganglion cell survival to delay diabetic retinopathy progress by targeting FGF5. *Bioscience, Biotechnology, and Biochemistry*, 83(9), 1655-1662. <http://dx.doi.org/10.1080/09168451.2019.1630251>. PMID:31272285.
- Zhou, X., Yao, Q., Sun, X., Gong, X., Yang, Y., Chen, C., & Shan, G. (2017). Slit2 ameliorates renal inflammation and fibrosis after hypoxia-and lipopolysaccharide-induced epithelial cells injury in vitro. *Experimental Cell Research*, 352(1), 123-129. <http://dx.doi.org/10.1016/j.yexcr.2017.02.001>. PMID:28163057.